

SELF-ASSEMBLED MONOLAYERS AND MODE-MIX DEPENDENT TRACTION-SEPARATION LAWS FOR INTRINSIC INTERFACIAL FRACTURE

Kenneth M. Liechti¹ and Alberto W. Mello²

¹Research Center for the Mechanics of Solids, Structures and Materials, The University of Texas at Austin, Austin, TX 78712

²CTA/IAE/ASA-G, Pr. Mal. Eduardo Gomes, 50, Sao Jose Dos Campos, SP, 12228-901 BRASIL

ABSTRACT

The purpose of the present study was to examine the effect of controlled adhesion on mixed-mode interfacial fracture toughness envelopes. The degree of adhesion was controlled by varying the areal density of the reactive tail groups of self-assembled monolayers (SAM) in sapphire/SAM/epoxy/aluminum sandwiches. The specimens were loaded in a new biaxial delamination tester that provided independent control of the mode-mix. The fracture envelope varied with mode-mix as has been seen before. For the bare sapphire substrates in the present study and glass/epoxy interfaces in previous studies, the intrinsic toughness was independent of mode-mix and the increase in toughness with increasing shear component was due to viscoplastic dissipation in the epoxy. However, coating the sapphire substrates with mixtures of SAM, gave rise to much higher intrinsic toughness values as the ratio of the more reactive group was increased. In addition, the intrinsic toughness or the traction-separation law varied with mode-mix, to the extent that no viscoplastic dissipation was excited in the epoxy over the range of mode-mixes that was considered.

1 INTRODUCTION

In studies of mixed-mode fracture near glass/epoxy interfaces, Swadener and Liechti [1] found that the increase in toughness with increasing shear was mirrored by an increase in the viscoplastic dissipation in the epoxy in a region outside the fracture process zone. The steady state toughness envelope was shifted vertically from the viscoplastic dissipation by a quantity that was identified as the intrinsic toughness of the interface. Because the viscoplastic dissipation was essentially zero under mode 1 conditions, the values of intrinsic and steady state toughness were the same. The intrinsic toughness was about 2 J/m² for this interface, making it about 20 times higher than the thermodynamic work of adhesion between glass and epoxy, as determined from contact angle and contact mechanics measurements and analyses [2]. This difference was accounted for by first noting the formation of highly localized ridges on the epoxy fracture surface. In addition, angle resolved X-ray photoelectron spectroscopic analyses of the glass fracture surfaces indicated that the cracks actually grew in the epoxy anywhere from 0.5 to 3 nm from the glass surface. This would be well within the so called interphase region in the epoxy where the properties differ from those of the bulk material [3-6]. Given the amorphous nature of the glass and the disorder in the interphase region, the present study was motivated by the desire to examine interfacial fracture under more carefully controlled conditions. As a result, sapphire substrates have been used along with mixtures of self-assembled monolayers with a view to providing adhesion control between the substrate and a thin layer of epoxy.

Polymeric self-assembled monolayers generally form covalent bonds with surface on which they are deposited. Self-assembly is usually a consequence of dense packing [7] of the molecules on the substrate. As a result, the head group at the other end of the chain may have a range of interactions with the material deposited on top of the monolayer. Depending on the materials involved, the interactions may be strong (covalent, ionic, hydrogen bonding or polar) or weak (non polar) in nature. One form of adhesion control can be achieved by making use of mixed SAMs where the head groups of each SAM have very different interactions with the material above [8, 9].

Zhuk et al. [8] used methyl (CH₃) and carboxy (COOH) terminal groups on 15-carbon alkanethiols to control adhesion between gold and epoxy. The thermodynamic work of adhesion of epoxy on the coated surface was linearly proportional to the COOH/CH₃ fraction in solution up to about 80%, and was constant thereafter. A series of superlayer fracture experiments revealed that the interfacial fracture toughness increased strongly with the thermodynamic work of adhesion. The rate of toughening increased with the work of adhesion, suggesting that more and more plastic dissipation was excited in the epoxy layer. Kent et al. [9] used mixed monolayers of dodecyltrichlorosilane (DTS) and bromo-undecyltrichlorosilane (BrUTS) to control adhesion between aluminum and epoxy. Both make strong covalent bonds with the aluminum. The methyl terminal group on the DTS again makes weak, non-polar interactions with the epoxy. The authors indicate that the BrUTS forms an alkyl ammonium bromide compound with the amine

crosslinker that was used to cure the EPON 828 epoxy. As a result, an ionic bond was achieved with the epoxy through $R-NH_2^+Br^-R'$ bonds. Between 10 and 20% bromine termination, there was a strong increase in the tensile and shear strengths of the aluminum/epoxy interface as determined by cruciform and napkin ring shear experiments. Asymmetric double cantilever experiments were used to determine the toughness of the interface, which increased linearly with the bromine fraction. The linear relationship was ascribed to the linear increase in the thermodynamic work of adhesion with bromine fraction [10]. In contrast to the gold/epoxy experiments, any plastic dissipation effects were apparently the same for all bromine fractions, even though the toughness of the aluminum/BrUTS/DTS/epoxy was much higher than that of the gold/COOH/CH3/epoxy interface in moist environments. The mode-mix in the asymmetric double cantilever beam experiments was -8° at a reference length of $10 \mu\text{m}$, whereas it was about 50° in the superlayer experiments.

The objective of the present study was to examine the interfacial toughness envelopes of quartz/epoxy, sapphire/epoxy and sapphire/SAM/epoxy interfaces. Fracture and toughening mechanisms were examined via crack opening interferometry, angle resolved X-ray photoelectron spectroscopy, atomic force microscopy and finite element analyses that accounted for the viscoplastic nature of the epoxy and adhesive interactions across the interfaces via traction-separation laws.

2 EXPERIMENTS

The loading device and experimental procedures that were used in this work have already been described [11]. A biaxial loading device capable of controlling displacements normal and tangential to the bondline to within 10 nm was used to load sandwich specimens (Fig. 1). They were made of aluminum 2024-T3 bonded to sapphire. The epoxy bond layer thickness h_2 was nominally $250 \mu\text{m}$. The exact thickness of the bond layers was measured after each experiment. The epoxy was a Bisphenol A resin cured with amido amine (CIBA-GEIGY products Araldite GY502 and Aradur HY955-1, respectively). The two components were mixed with a weight ratio of 100:40 resin to hardener and placed in a vacuum chamber for about 15 minutes to remove bubbles and solvents. The epoxy mixture was then injected into a mold containing the two substrates that were held at a fixed distance apart [12]. The epoxy was cured for at least 7 days at room temperature.

The aluminum face which was to be bonded was polished with 600 grit sand paper and treated with a chromic acid etch for 5 minutes at room temperature. The surface was then cleaned with acetone. The sapphire, when used as received, was only cleaned with acetone and optical tissue. When used with SAMs, the sapphire was cleaned with a "piranha etch", which is a solution of 98% H_2SO_4 (sulfuric acid) and 30% H_2O_2 (hydrogen Peroxide) in volume ratios of 2-4:1. The solution was used at a temperature of 130°C , for 15 minutes. The surfaces were then rinsed with de-ionized water and dried in a dry nitrogen stream.

A mixture of two SAMs was considered for controlling the surface interactions between the epoxy and the substrates. The SAMs were dodecyltrichlorosilane, $CH_3(CH_2)_{11}SiCl_3$, and bromo-undecyltrichlorosilane $Br(CH_2)_{11}SiCl_3$, designated DTS and BrUTS, respectively. In both cases the Cl reacts with the sapphire to form a covalent bond between the Si and Al_2O_3 . The terminal groups of DTS and BrUTS have weak and strong interactions, respectively, with the epoxy. As a result, the degree of adhesion was controlled by altering the ratio of BrUTS to DTS [9]. The ratios considered in this work were 0, 10, 55 and 70% by volume of BrUTS. The reason for mixing DTS and BrUTS was that their chain lengths are quite similar, which discourages island formation. Following the piranha etch, the dried sapphire was subjected to a 15 second flame anneal [13]. The sapphire was then submerged for 5 hours at 60°C in a hexadecane solution containing a mixture of DTS and BrUTS in a volume ratio of 5 drops of the SAM for each 20 ml of anhydrous hexadecane. The coated sapphire was sonicated in toluene for 20 minutes to remove clusters and then blown dry with a stream of dry nitrogen [9]. Contact angles increased [12] with increasing amounts of BrUTS following the trends given in [10].

Crack opening displacements were measured to within 30 nm up to 300 nm from the crack front using crack opening interferometry. The epoxy fracture surface was imaged with an atomic force microscope. The sapphire fracture surface was interrogated with angle resolved X-ray photoelectron spectroscopy. Details of all these measurements are given in [12].

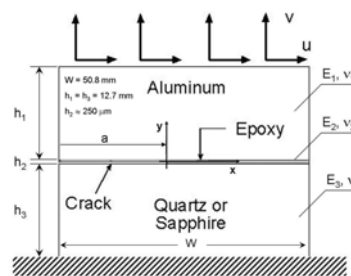


Figure 1. Specimen geometry and loading.

3 ANALYSIS

There were several components to the analytical/numerical aspects of the work. First, the energy release rate and fracture mode-mix were determined from the measured displacements normal and tangential to the bondline. The traction-separation law and the viscoplastic dissipation associated with each interface were extracted from finite element analyses, whose solutions were matched with measured values of crack opening displacements.

The energy release rate during steady state propagation was obtained from

$$G = \frac{v^2}{2} \left(\frac{h_1}{\hat{E}_1} + \frac{h_2}{\hat{E}_2} + \frac{h_3}{\hat{E}_3} \right) + \frac{u^2}{2} \left(\frac{h_1}{\mu_1} + \frac{h_2}{\mu_2} + \frac{h_3}{\mu_3} \right). \quad (1)$$

where v and u are the applied displacements normal and tangential to the bondline, h_i are the heights of the sapphire, epoxy and aluminum, respectively and \hat{E}_i and μ_i are the reduced tensile and shear moduli. The fracture mode-mix angle was

$$\psi = \tan^{-1} \frac{K_2}{K_1} + \varepsilon \ln \left(\frac{\hat{l}}{h_2} \right). \quad (2)$$

The stress intensity factors were obtained from

$$K_1 + iK_2 = h_2^{ic} e^{i\omega} \left(\frac{E_*}{1 - \beta^2} \right)^2 \left[\frac{v}{\sqrt{2}} \left(\frac{h_1}{\hat{E}_1} + \frac{h_2}{\hat{E}_2} + \frac{h_3}{\hat{E}_3} \right)^{-1/2} + i \frac{u}{\sqrt{2}} \left(\frac{h_1}{\mu_1} + \frac{h_2}{\mu_2} + \frac{h_3}{\mu_3} \right)^{-1/2} \right]. \quad (3)$$

where β is one of the Dundurs parameters and ω depends on the elastic properties of all three materials and differed [1] from the results for a two material sandwich [14] by one degree.

The stresses in the sapphire, quartz and aluminum were far below yielding for any combination of mode-mix. Consequently, these materials were considered to be linearly elastic in the finite element analyses that follow. The epoxy was subjected to very high stress levels in the vicinity of the crack tip. In addition, as the crack advanced, the plastic strain rate varied ahead of and inside the plastic zone. The mechanical behavior of the epoxy was accounted for using a power law rate dependent plasticity model.

The rate dependence of the epoxy [12] is shown in Figure 2. The viscoplastic model uses the Mises yield surface with associated plastic flow and isotropic hardening. The rate dependence was accounted for by interpolation and extrapolation of data at different rates. This combination allows the hardening curve to accommodate local variations in strain rate. The equivalent plastic strain is given by:

$$\varepsilon_e^{pl} = \varepsilon_e^{pl} \Big|_t + \int_t^{t+\Delta t} \sqrt{\frac{2}{3}} \dot{\varepsilon}_e^{pl} : \dot{\varepsilon}_e^{pl} dt \quad (4)$$

and the equivalent stress is obtained by a power law rate dependence:

$$\frac{\sigma_e(\varepsilon_e^{pl}, \dot{\varepsilon}_e^{pl})}{\sigma^0(\varepsilon_e^{pl})} = \left(\frac{\dot{\varepsilon}_e^{pl}}{\dot{\varepsilon}_0^{pl}} \right)^m \quad (5)$$

For the current work, the rate dependence in the true uniaxial stress-strain behavior was based on data given in Figure 2, which has a rate exponent $m = 0.076$. The stresses at other rates were interpolated by the ABAQUS[®] solver.

The plastic dissipation was obtained as the plastic work consumed during a period of crack advance, which is given by:

$$\Delta W_p = \int_{\Omega} \underline{\sigma} \bullet \Delta \underline{\varepsilon}_p d\Gamma \quad (6)$$

where Ω is the contour which encircles all elements that deformed plastically. The total value of the plastic work can be obtained directly from the energy dissipated by rate-dependent plastic deformation in each computational step as a function of the crack length. The plastic dissipation component of the energy release rate is given by:

$$G_p = \frac{1}{b} \frac{\Delta W_p}{\Delta a} \quad (7)$$

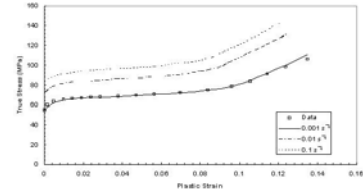


Figure 2. Plane strain compression behavior of the epoxy.

where b is the width of the specimen and Δa is the crack increment.

A cohesive zone model was used to represent the fracture process zone in finite element analyses of steadily propagating cracks. In the analyses, the crack speed was taken to be the average of the crack speeds observed in the experiments. In addition, once the crack tip reached a node, the tractions were released linearly with time as the crack advanced. The size of the cohesive zone α was adjusted to match the numerical solution for NCO with the measured values. The relative displacements of the crack faces were then obtained from the solution. This scheme resulted in an approximately linear relationship between the tractions and relative displacements of the crack surfaces. In the absence of direct measurements, this traction-separation law was adequate for modeling fracture in these experiments, especially since it has been shown that the shape of the traction-separation law does not significantly affect the fracture toughness [1, 15]. In order to properly represent steady state crack propagation, the crack was allowed to grow for several cohesive zone lengths.

4 RESULTS and DISCUSSION

The crack speed was measured from the video recording of the fringe patterns from the crack opening interferometer [12]. In the experiments with bare sapphire specimens, the average crack speed under steady state conditions was 5.0 $\mu\text{m/s}$. For the experiments with the SAM coated-sapphire, the average crack speed was 3.5 $\mu\text{m/s}$. The crack speed was used as input to the finite element analysis. Its value was particularly important for establishing the strain rate at the crack tip.

The applied displacements during steady state crack growth were used in equations (1), (2) and (3) for determining energy release rates and phase angles. The results for the current experiments are shown in Figure 3. All data sets refer to an arbitrary length scale parameter of 1 μm . For the sapphire experiments, there was a higher degree of scatter in the steady state energy release rate from specimen to specimen. The sapphire surface was more susceptible to slight changes possibly introduced by reuse of specimens. To minimize this scatter, the sapphire was cleaned with piranha etch before reuse. The intrinsic toughness of the bare sapphire/epoxy interface was slightly lower than that of the glass/epoxy interface [1]. Completely different levels of steady state toughness were obtained when the sapphire was coated with mixed monolayers (Fig. 3). It can be seen that the minimum toughness of the coated-sapphire was 4.5 and 5 times greater than that of the bare sapphire for 10%BrUTS and 55%BrUTS, respectively. This increase in toughness is due to the bonding produced by the terminal bromine atoms with the epoxy through specific local interactions [9]. The methyl terminal groups of DTS only bond with the epoxy through non local van der Waals interactions [9]. The higher toughness led to a much sharper minimum in the fracture toughness envelope and suggests that a significant amount of plastic dissipation was occurring even under mode 1 conditions. Such changes in the shapes of the fracture toughness envelopes were predicted [15]. The toughness of a specimen made with 70% BrUTS coated-sapphire was so high that it was not possible to initiate a single crack at the interface [12]. The adhesion between the sapphire and the epoxy was such that voids nucleated at multiple sites instead. Some void growth also occurred between the epoxy and the aluminum.

The experiments were analyzed with finite elements. As indicated earlier, the scheme that was used to implement a cohesive zone analysis had the cohesive zone size as a free parameter. The proper cohesive zone size was chosen by matching the numerical solutions

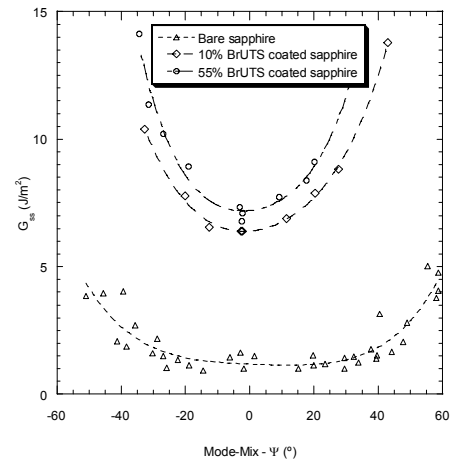


Figure 3. Mixed-mode toughness envelopes for bare and coated sapphire

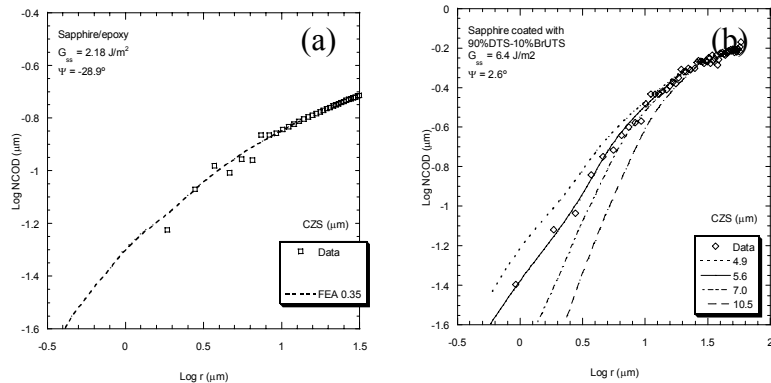


Figure 4. Normal crack opening displacements used to determine cohesive zone size. (a) bare and (b) coated sapphire.

for the NCOD with the measured values. Figures 4a,b show, respectively, the trial of one and four different cohesive zone sizes for bare sapphire/epoxy and coated sapphire/epoxy specimens. As can be seen, cohesive zone sizes of $0.35\ \mu\text{m}$ and $5.6\ \mu\text{m}$ are the ones that provided the best agreement with the measured NCOD for the bare and coated-sapphire/epoxy interfaces, respectively. The much larger cohesive zone for the coated-sapphire is in agreement with the trend in the toughness envelopes (Fig.3).

The traction-separation laws for the analyses that produced the solutions of Figure 4 are shown in Figure 5. The traction-separation laws are plotted as the vector magnitudes of the tractions and crack opening displacements. For the bare sapphire, the intrinsic fracture toughness (area underneath the traction-separation laws) was the same for all mode-mixes. The maximum traction (Fig. 5a) was about 120 MPa, which was higher than any of the plateau levels shown in Figure 2. This is due to the fact that the strain rates near the crack tip were higher [12] than any of the values shown there. Nonetheless, it appears that the maximum traction was similar to the yield strength of the epoxy. This was lower than the range of values (from 2 to 8 times the yield strength) that were used in earlier analyses [15] of interfacial crack growth.

In contrast to the results just presented for the bare sapphire specimens, the traction-separation laws for the sapphire specimens coated with 10%BrUTS varied considerably with mode-mix [Fig. 5b]. First, it can be seen that the traction-separation law for $\Psi = -2.6^\circ$ was highly non-linear and had the lowest intrinsic fracture toughness. As the mode-mix increased, the traction-separation law became more linear and the intrinsic toughness increased with increasing mode-mix, something that we had never seen in previous experiments with the glass/epoxy interfaces [1] and the bare sapphire (and quartz [12]) specimens that were used in this study. In addition, it can be seen that the maximum levels of vector traction for the coated sapphire were about two thirds of the values that were seen (Fig. 5a) for the bare sapphire. These lower maximum traction levels suggest that very little yielding was occurring outside the cohesive zone. At the same time, the maximum values of VCOD were about ten times larger than the values for the bare sapphire. This is consistent with the much larger cohesive zone size of the coated sapphire specimens (Fig. 4).

Values of steady state toughness and plastic dissipation were computed as described in Equations (1, 2, 6 and 7). Figure 6a shows the values of toughness and plastic dissipation for the bare sapphire/epoxy interface, as a function of the mode-mix. For mode-mixes between -5 and 20° , the plastic dissipation was much less than the toughness, which implies that the intrinsic toughness was the toughness in that range. For larger mode-mixes, the rise in toughness was mirrored by the dissipation as had been noted for glass/epoxy interfaces [1]. Note that the closed form and numerical solutions for the toughness were in good agreement. A similar series of analyses were conducted for the sapphire specimens that were coated with 10% BrUTS. As was noted earlier (Fig. 3), this relatively small amount of BrUTS raised the minimum toughness over the intrinsic toughness of the bare sapphire by a factor of 4.5. Our first thought was that this was due to an increase in plastic dissipation even under mode 1

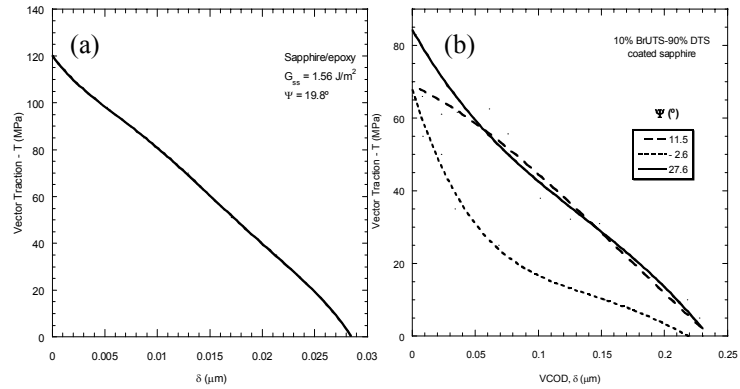


Figure 5. Traction separation laws for (a) bare and (b) coated

sapphire. Values of steady state toughness and plastic dissipation were computed as described in Equations (1, 2, 6 and 7). Figure 6a shows the values of toughness and plastic dissipation for the bare sapphire/epoxy interface, as a function of the mode-mix. For mode-mixes between -5 and 20° , the plastic dissipation was much less than the toughness, which implies that the intrinsic toughness was the toughness in that range. For larger mode-mixes, the rise in toughness was mirrored by the dissipation as had been noted for glass/epoxy interfaces [1]. Note that the closed form and numerical solutions for the toughness were in good agreement. A similar series of analyses were conducted for the sapphire specimens that were coated with 10% BrUTS. As was noted earlier (Fig. 3), this relatively small amount of BrUTS raised the minimum toughness over the intrinsic toughness of the bare sapphire by a factor of 4.5. Our first thought was that this was due to an increase in plastic dissipation even under mode 1

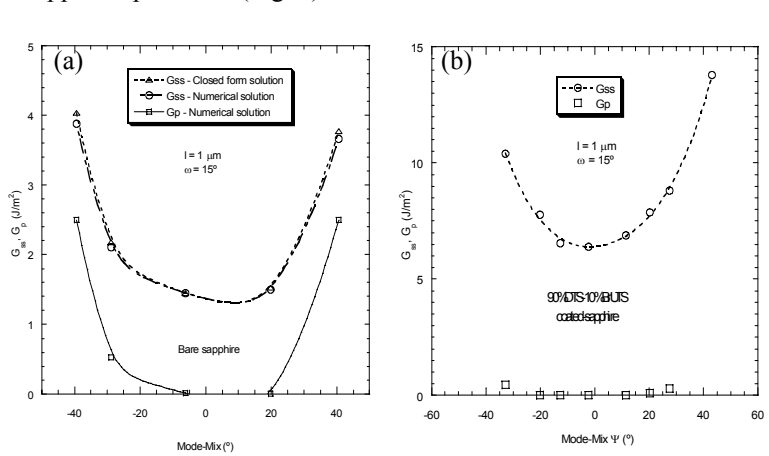


Figure 6. Toughness and plastic dissipation (a) bare and (b) coated sapphire

Mode 1

conditions. However, the results (Fig. 6b) show that there was very little plastic dissipation outside the cohesive zone over the range of mode-mixes that could be analyzed. It was not possible to obtain convergent solutions for mode-mixes beyond those shown. Nonetheless, it is already apparent that the plastic dissipation did not track the toughness as was the case for bare sapphire or quartz [12] or glass [1]. The increase in toughness for the coated sapphire was mainly accounted for by the increase in intrinsic toughness brought about by the different amounts of BrUTS. As indicated above (Fig. 5), this intrinsic toughness was not independent of mode-mix.

The differences in behavior noted in Figures 3-6 above were related [12] to differences in the appearance of the epoxy fracture surfaces and the amount of epoxy remaining on the sapphire fracture surfaces as respectively detected by atomic force microscopy and angle resolved X-ray photoelectron spectroscopy. For bare sapphire, crack growth occurred by a lateral tunneling mechanism [2] that left ridges on the epoxy fracture surface. For coated sapphire, crack growth was accompanied by ligament formation, probably related to the strong bonding sites provided by the Br groups on the BrUTS. There was more epoxy left on the sapphire fracture surfaces when the sapphire had been coated with BrUTS.

5 CONCLUSIONS

Coating the sapphire with mixtures of the self-assembled monolayers, BrUTS and DTS, provided much higher levels of sapphire/epoxy interfacial toughness. The character of the mixed-mode fracture toughness envelopes also changed. The traction-separation law for bare sapphire was independent of mode-mix and the increase in toughness with mode-mix was related to plastic dissipation in the epoxy. However, the traction-separation laws for the specimens with coated sapphire completely accounted for the increase in toughness with mode-mix, thereby providing a unique example of intrinsic toughness varying with mode-mix.

6 REFERENCES

1. Swadener, J. G. and Liechti, K. M. (1998), "Asymmetric shielding mechanisms in the mixed-mode fracture of a glass/epoxy interface". *Journal of Applied Mechanics*, **65**, 25-29.
2. Swadener, J. G., Liechti, K. M. and Lozanne, A. L. (1999), "The intrinsic toughness and adhesion mechanisms of a glass/epoxy interface". *Journal of the Mechanics and Physics of Solids*, **47**, 223-258.
3. Drzal, L. T. (1986), "The interphase in epoxy composites." *Advances in Polymer Science*, **75**, 1-32.
4. Drzal, L.T. (1990), "The role of the fiber/matrix interphase on composite interfaces", *Vacuum*, **41**, 1615-1618.
5. Winter, R.M. and Houston, J.E. (1998a), "Interphase Mechanical Properties in an Epoxy-Glass Fiber Composites as Measured by Interfacial Microscopy," in *Proceedings of the SEM Spring Conf. on Exp. and Applied Mechanics*, Houston, TX, June 1-3, 1998.
6. Winter, R.M. and Houston, J.E. (1998b), "Nanomechanical Properties of the Interphase in Polymer Composites as Measured by Interfacial Force Microscopy," presented at the *Mat. Res. Soc. Spring Meeting*, San Francisco, CA, April 13-17, 1998.
7. Kojio, K., Ge, S., Takahara, A. and Kajiyama, T. (1998), "Molecular aggregation state of *n*-octadecyltrichlorosilane monolayer prepared at an air/water interface," *Langmuir*, **14**, 971-974.
8. Zhuk, A. V., Evans, A. G., Hutchinson, J. W. and Whitesides, G. M. (1998), "The adhesion energy between polymer thin films and self-assembled monolayers," *Journal of Materials Research*, **13**, 3555-3564.
9. Kent, M. S., Yim, H., Sorenson, J., Matheson, A., Reedy, E. D. and Majumdar, B. (2003), "Using self-assembled monolayers to explore the relationships between interfacial interactions and fracture in structural adhesive joints," *Proceedings of the 23rd Annual Adhesion Society Meeting*, 323-325.
10. Reedy, E.D., Kent, M.S. and Moody, N. R. (2003), "On the relationship between the molecular work of separation and interfacial fracture toughness," *Proceedings of the 23rd Annual Adhesion Society Meeting*, 502-504.
11. Mello, A. W. and Liechti, K. M. (2003), "A piezoelectric biaxial loading device for interfacial fracture experiments". Submitted to *Experimental Mechanics*. Engineering Mechanics Laboratory Report EMRL 03/10.
12. Mello, A. W. (2003), "Mode-mixed fracture experiments on quartz/epoxy and sapphire/epoxy interfaces". Doctoral Dissertation. The University of Texas at Austin. Department of Aerospace Engineering and Engineering Mechanics. Engineering Mechanics Laboratory Report EMRL 03/11.
13. Eng, P. J. (2000), "Structure of the hydrated α -Al₂O₃ (0001) surface". *Science*, **288**, 1029-1033.
14. Hutchinson, J. W. and Suo, Z. (1992), "Mixed-mode cracking in layered materials". *Advances in Applied Mechanics*, **29**, 63-191.
15. Tvergaard, V. and Hutchinson, J. W. (1993) "The influence of plasticity on mixed-mode interface toughness." *Journal of the Mechanics and Physics of Solids*, **41**, 1119-1135.